

# ELECTRIC SPARK DISCHARGE IN AIR CHARACTERIZATION BY FOLLOWING ELECTRODES EROSION

S. BERNARD<sup>1\*</sup>, S. PELLERIN<sup>2\*</sup>, P. GILLARD<sup>1</sup>, D. ASTANEI<sup>2,3</sup>

<sup>1</sup> PRISME, Orleans University 63 avenue de Lattre de Tassigny, 18020 Bourges, France

<sup>2</sup> GREMI Laboratory, Orleans University/CNRS, Bourges, 18028, France

<sup>3</sup> „Gheoghe Asachi“ Technical University of Iasi, Iasi, 700050, Romania

\* [stephane.bernard@univ-orelans.fr](mailto:stephane.bernard@univ-orelans.fr), [stephane.pellerin@univ-orleans.fr](mailto:stephane.pellerin@univ-orleans.fr)

## ABSTRACT

The plasma column diagnosis of an electric discharge used to ignite dust explosion, has been performed by optical emission spectroscopy methods using the well-known Boltzmann plot method based on W I spectral lines, to determine the electron temperatures. In the peripheral zone of the discharge, molecular spectroscopy methods are applied, by comparing the experimental spectrum with a simulated one.

The first results indicate that the plasma is close to the local thermodynamic equilibrium at a temperature close to 11000 K.

## 1. INTRODUCTION

Dust explosion hazard management is usually achieved by characterizing the sensibility of combustible dust to ignition and the severity of their explosion in the air. The characterization requires the measurement of data such as MIE [1], TMI,  $P_{\max}$  Kst,... Most of ignition sources are due to electrostatic discharge and it is for that reason that the MIE (Minimum Energy of Ignition) is measured in an apparatus where explosion is ignited with an electric discharge after the generation of a dust cloud in a closed Hartmann tube. MIE is determined with statistical method [2] requiring only an electrical calibration of the electric discharge and provides enough data's for risk assessment, but in no cases allows to describe ignition phenomena at the dust scale when it gone into the electric spark. In this way this study concern the characterisation of the electric discharge (the measurement of the temperature field) in a first time in order to dispose of realist data's for a better understanding of interaction phenomena between dust and the electric discharge.

## 2. PRELIMINARY OBSERVATIONS

### 2.1. The power supply

The power supply is designed to produce an arc at nearly constant power (voltage and current intensity are constant) and a scheme of the electric circuit is given in figure 1. Energy, in such a case, is only proportional to the duration of the spark. This time could be changed over the range of 1  $\mu$ s to 100 ms. The proper, breakdown of the arc is preceded by a pulse of high voltage helping to initiate the low voltage spark. The pulse shape is shown in figure 2. The arc energy value achieved with such an arrangement is in the range from 4 mJ to 50 J, making it possible to measure the ignition energy of the less ignitable dusts.

Our experiments have been made with fixed duration time to  $\tau = 50 \mu$ s, with mean arc voltage close to 90 V, and courant discharge around 3.7 A. The tests were performed in air at atmospheric pressure.

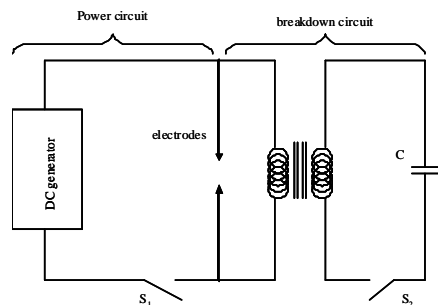


Figure 1. Scheme of the spark generator supply

### 2.2. Electrical parameters

In order to determine the energy consumed by the discharges produced by the spark device and also to identify the lifetime of the sparks, the

current of the discharge has been measured using a current transducer (0.1V/A), and a voltage divider with a rapport of transformation 1/10 has been used for voltage measuring. These electrical characteristics were stored using numerical oscilloscope LECROY Wavesurfer 64MXs-A (bandwidth 600 MHz, 5 GS/s, 16 Mpts/Ch).

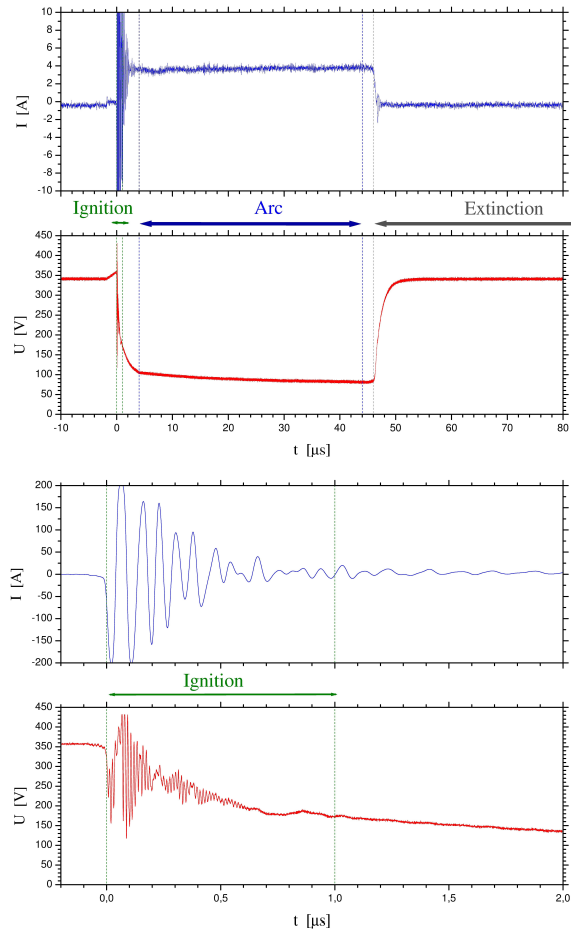


Figure 2. Spark discharge electrical parameters.

A typical record of the electric parameters is shown in Figure 2. Then, we can divide the spark's lifetime into three periods: at the breakdown time, during approximately  $\tau_{\text{ignition}} = 2 \mu\text{s}$ , there are significant variations in the discharge current and voltage, certainly linked to a reaction of the power supply; then, about  $t_d = 4 \mu\text{s}$  after the start of the ignition, the plasma seems to stabilize for about  $\tau_{\text{arc}} = 40 \text{ms}$ . Extinction comes next, followed by a plasma in extinction that endures a few tens of ms.

### 2.3. Plasma evolution

The evolution of the spark was followed by high speed cinematography (exposure time of  $t_{\text{exp}} = 10 \text{ns}$ , to time steps  $\Delta t_d = 50\text{ns}$ ) using an

ICCD camera (Cf. Figure 3). The luminosity of the plasma column varies significantly in the first instants of the discharge, in accordance with the observed voltage and current variations. Then it stabilizes during the duration of the period defined by  $\tau_{\text{arc}}$  above. Finally, the extinction of the discharge widely extends after the end of the electric pulse, until approximately  $t_d \approx 200 \text{ms}$  after the start of the pulse.

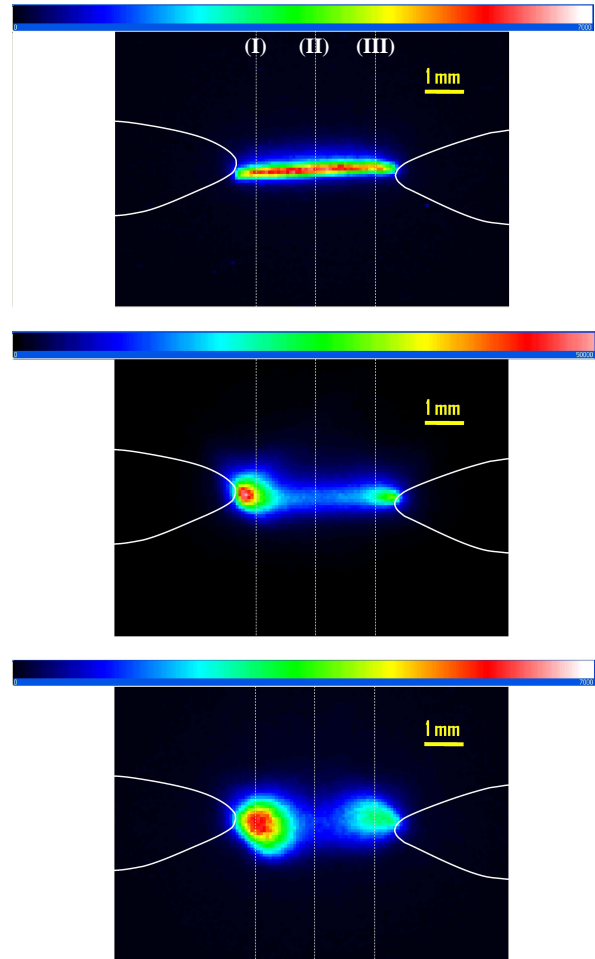


Figure 3. Spark discharge evolution: a- ignition time ( $t_d=50\text{ns}$ ,  $t_{\text{exp}}=550\text{ns}$ ); b- arc ( $t_d=4\mu\text{s}$ ,  $t_{\text{exp}}=40\mu\text{s}$ ); c- extinction ( $t_d=46\mu\text{s}$ ,  $t_{\text{exp}}=90\mu\text{s}$ ). Dashed lines indicate the optical line sights.

In the present study, we will study the plasma in the intermediate phase, which seems in quasi-steady state, between  $t_d = 4 \mu\text{s}$  and  $44 \mu\text{s}$  after ignition.

## 2. EXPERIMENTAL PROCEDURE

### 2.1. Spectroscopical set-up

The spectroscopic analysis of the electrical discharges produced in air was done with the experimental set-up shown in figure 4. An ACTON 750i spectrometer (ROPERS

Scientifics, 750 mm focal length, resolution lower than 0.1 nm) equipped with two-dimensional intensified charge-coupled device (ICCD) camera (512×512 pixels) has been used. The plasma image was focused directly on the entrance slit (set to 5 μm) of the spectrometer using a quartz lens (focal length  $f \approx 10$  cm) with an enlargement factor equal to 3. The spark's device was placed on a step-by-step moving device to allow study of the different regions of the discharge. The space between the spark plug electrodes was divided into three areas of analysis (see dashed lines on Figure 3): near high voltage electrode (cathode – zone I), near the grounded electrode (anode – zone III) and in the center of the plasma column (zone II). No radial exploration of the discharge was performed in this study, and the records refer to the space around the high voltage electrode. The distance between the electrodes was 4 mm.

The exposure time of the OMA-ICCD camera was chosen (40 μs, with a delay of 4 μs after the ignition) to allow to record spectra corresponding to the total lifetime of the sparks (see precedent section), so to calculate an “averaged temperature” in time. The spectra are side-on recorded, and provide data easier to be processed.

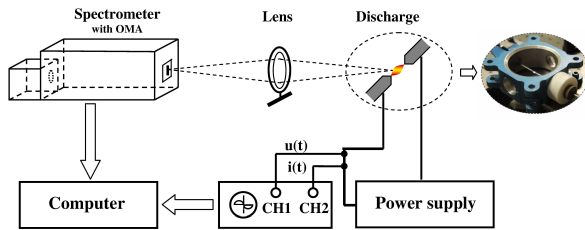


Figure 4 Spectroscopic set-up for the discharge.

The arc spectrum has been recorded between 200 and 900 nm and revealed many intensive W I lines, but also ionized wolfram lines especially in the zone near the cathode. Some lines of atomic nitrogen are also present, as well as the well known O I triplets near 777 nm and 844 nm. Furthermore, the head of bands at 388.34 nm of CN violet spectrum appears clearly in the column, as well as, under particular conditions, the head of band at 391.44 nm of the second negative system of molecular nitrogen and the UV OH molecular spectrum at 306.36 nm. It should be noted the presence of a large number of unidentified lines, probably due to the metallic impurities of the cathode.

## 2.2. Determination of the electronic temperature

The intensive W I lines can be used to determine the excitation temperature using the atomic Boltzmann plot method [3]. Assuming the LTE state, the plasma temperature can be obtained by plotting the equation

$$y \equiv \ln \left( \frac{\varepsilon_{ki} \lambda_{ki}}{A_{ki} g_k} \right) = \ln K - \frac{E_k}{k T_e} \quad (1)$$

where  $\varepsilon_{ki}$  is the line intensity,  $\lambda_{ki}$  is the wavelength and  $E_k$  and  $g_k$  are the excitation energy and statistical weight of the upper atomic state respectively;  $k$  is the Boltzmann constant and  $K$  is a constant for all the considered lines. Then, the slope of the straight line obtained is inversely proportional to the electronic temperature.

However, in our case, the intensity of several optically narrow lines of W I, in the wavelength region 200 – 900 nm, were recorded along a given line of sight chord in the plasma source. Application of the atomic Boltzmann method in such a case of spatially integrated measurements cannot give the central axis temperature without application of the Abel inversion technique.

In this technique, a plot of

$$y \equiv \ln \left( \frac{\varepsilon_{ki} \lambda_{ki} E_k}{A_{ki} g_k} \right) = \ln K - \frac{E_k}{k T_e} \quad (2)$$

as a function of  $E_k$ , gives the central axis temperature; in this case,  $\varepsilon_{ki}$  is the spatially integrated line intensity, and  $K$  is a constant for all W I lines. This expression differs from the well-known classical atomic Boltzmann plot method [4] by the presence of the energy term ( $E_k$ ) present in the logarithm.

Fifteen optically narrow W I lines were chosen in order to cover the maximum energy difference and to increase the precision of the method. The slope of the straight lines obtained is inversely proportional to the electronic temperature.

The accuracy of this method is quite close to that of the data available in the literature (15–30%, in [5]), and the method was sensitive in the determination of intensity of lines that were sometimes not well resolved. Particularly with a poor signal-to-noise ratio, the error in temperature can be higher than 2000 K. Nevertheless, this method gives a good estimate of the equilibrium plasma state, because points in the Boltzmann plots were then relatively well aligned (see example in figure 5).

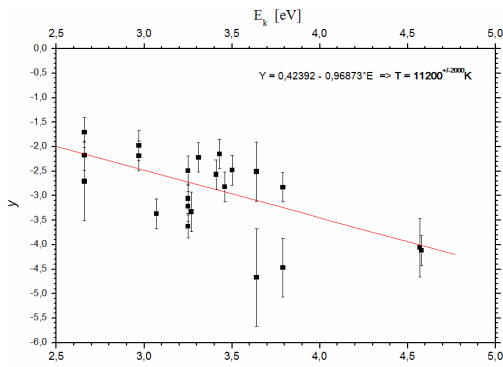


Figure 5. Modified Boltzmann Plot, close to the cathode

### 2.3. Determination of the rotational and vibrational temperatures

The values of the rotational temperature were obtained using optical emission method based on the comparison between experimental and theoretical rotational structures of the UV molecular emission spectra of the OH (A-X) band at 306.357 nm ( $\Delta v=0$ ). The first step of the method is the extraction of the spectra offset and the identification of the optical apparatus function. Taking into consideration the results, it is calculated the ratio between amplitudes of certain peaks of the spectra. This ratio indicates the rotational temperature  $T_R$ , [6].

To complete the obtained values, the experimental spectra have been fitted by using a specialized software, SPECAIR 3.0 [7, 8], especially in the range where  $N_2^+$  and CN molecular spectra were visible. To fit a spectrum the software takes in account parameters as electronic, rotational, translational and vibrational temperatures, the mole fractions of the molecular or atomic species presented into plasma and the apparatus functions.

## 3. RESULTS AND CONCLUSIONS

In the vicinity of the cathode, the modified Boltzmann plot indicates an excitation temperature around 11500 K on the axis of the plasma. On the other hand, the tungsten spectral lines are not usable in the zone (2), and the method cannot be used.

The use of molecular spectra, including that of OH, is made difficult by the presence of numerous superimposed metallic lines. Nevertheless, the results obtained with the software SPECAIR, give similar electronic, vibrational and rotational temperatures, close to 10500 K.

All these results seems to indicate that the plasma is close to the local thermodynamic equilibrium, and the resulting temperature can be used as an input parameter in the modeling of the explosions of dust generated in the laboratory. These results must now be complemented by a study of the spatial and temporal evolution of the plasma.

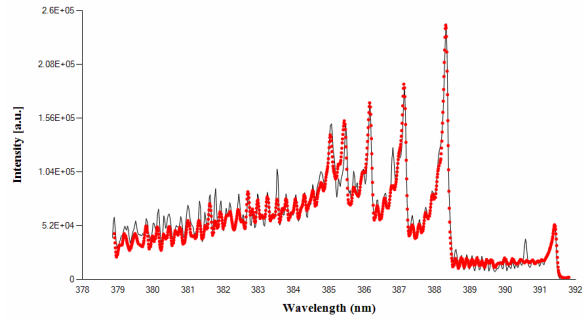


Figure 6. Molecular spectrum in the 380-392 nm spectral range, recorded in the column.

## REFERENCES

- [1] S.Bernard, P.Gillard, F.Foucher & C.Mounaïm, MIE and flame velocity of partially oxidised aluminium dust, *J Loss Prev Process Indust*, **25**-3, (2012) 460-466.
- [2] S.Bernard, K.Lebecki, P.Gillard, L.Youinou & G.Baudry, Statistical Method for the Determination of the Ignition Energy of Dust Cloud- Experimental Validation, *J Loss Prev Process Indust*, **23**-3(2010) 404-411.
- [3] J.Chapelle, L'arc électrique et ses applications: T.1 Etude physique de l'arc électrique, Ed Paris: CNRS (1984) 256-285
- [4] A.Marotta, Determination of axial thermal plasma temperatures without Abel inversion *J.Phys.D* **27** (1994) 268-272
- [5] NIST Atomic Spectra Database Data <http://physics.nist.gov>
- [6] S.Pellerin, J.-M.Cormier, F.Richard, K.Musiol & J.Chappelle, A spectroscopic diagnostic method using UV OH band spectrum, *J. Phys. D* **29** (1996) 726-739
- [7] SpecAir, <http://www.specair-radiation.net/>
- [8] C.O.Laux, Radiation and Nonequilibrium Collisional-Radiative Models, *von Karman Institute Lecture Series 2002-07*, Special Course on Physico-Chemical Modeling of High Enthalpy and Plasma Flows, eds. D.Fletcher, J.-M.Charbonnier, G.S.R.Sarma, and T.Magin, Rhode-Saint-Genèse, Belgium, 2002.